THE ASTROPHYSICAL JOURNAL, 214:179–188, 1977 May 15

OPTICAL EMISSION FROM SHOCK WAVES. III. ABUNDANCES IN SUPERNOVA REMNANTS

M. A. DOPITA, D. S. MATHEWSON, AND V. L. FORD
Mount Stromlo and Siding Spring Observatory, Research School of Physical Sciences, Australian National University
Received 1976 June 1; revised 1976 November 9

ABSTRACT

The diagnostic techniques described by Dopita have been applied to observations of many supernova remnants in our Galaxy and the Magellanic Clouds to yield abundances of oxygen, nitrogen, and sulfur. A strong gradient in chemical evolution is found, increasing from the SMC through the LMC to the Galaxy, consistent with theories of enrichment. An upper limit of 4×10^{-5} is placed on the pregalactic oxygen abundance, and no strong evidence is found to indicate galactic evolutionary dependence of enrichment processes. Evidence is presented to indicate that two objects observed could be fragments of the original supernova preferentially thrown off in a certain direction during the explosive event.

Subject headings: galaxies: Magellanic Clouds — nebulae: abundances — nebulae: supernova remnants — shock waves

I. INTRODUCTION

In Paper I of this series (Dopita 1976) we showed that, in at least one supernova remnant, N49 in the LMC, it is possible to derive fairly accurate abundances by fitting observed line intensities to those computed in a model of a plane-parallel radiating shock of modest velocity. Paper II (Dopita 1977) generalized these results to a large range of abundances and shock conditions, and a set of diagnostic diagrams analogous to those used for many years in interpreting H II region spectra were given. We will now use these diagrams to attempt to compute these quantities from image-tube spectra obtained on the Cassegrain spectrograph of the 74 inch (1.9 m) at Mount Stromlo, from spectra using the IDS on the 150 inch (3.8 m) Anglo-Australian Telescope at Siding Spring, and from high-quality data already available in the literature (Parker 1967; Osterbrock and Costero 1973; Osterbrock and Dufour 1973; D'Odorico 1974). Remnants observed in the clouds were selected from those identified previously by Mathewson and Clarke (1973*a*, *b*, *c*) from the radio spectrum and the strength of the [S II] lines.

Abundances derived from these spectra represent a valuable complement to those obtained from observations of H II regions and planetary nebulae as indicating the stage to which enrichment processes have evolved in our Galaxy and the Magellanic Clouds.

II. OBSERVATIONS AND THEIR REDUCTION

The image-tube spectra presented here represent a homogeneous set of observations made in 1972 June and October. The dispersion used was 100 Å mm^{-1}, and exposures ranged between 30 minutes and 2 hours. To reduce observational uncertainty as far as possible, only those plates for which all lines occurred on the linear portion of the density/intensity relationship have been used.

Osterbrock and Dufour (1973) have made very high-quality observations of one region in N49; and since our own spectra have this region in common, we have used their published intensities as a standard to calibrate our observations. This has the advantage that line ratios of our program objects do not differ by very large factors from this region, nor do exposure times; so intensity-dependent errors are reduced to a minimum.

Since our spectra did not extend down to Hγ, reddening corrections have been made on the assumption that the ratio of Hα and Hβ is 2.9. This value was obtained from the computed recombination temperature obtained from the theoretical shock models, using effective recombination coefficients given by Brocklehurst (1971) for case B. The variation in recombination temperature found in the models would alter this ratio only by 10%. Collisional excitation of Hα is ignored, as Cox (1972) has shown that it makes only a few percent change, less than our observational errors.

The observed line intensities and their values corrected for reddening are shown in Table 1. Although intensities are given to (in some cases) three figures, we expect that errors in ratios of adjacent lines may be as large as 15% and, for well-separated lines including reddening corrections, may well be as large as 25%.

The intensities of the [O I] lines may have larger errors than this, however. This is because the sky background is in some instances very strong compared with the nebula. The correction for sky background was determined by finding the faintest region of nebulosity along the slit length and subtracting this from the main signal. Then in many cases the observed spectrum is bright nebulosity plus sky minus faint nebulosity plus sky, and such a procedure may change relative line intensities. In particular, it will reduce the [O I] intensities with respect to Hβ. However, it is the best we can do, since the sky spectrum cannot be separately observed because of its variability.

The observations on the 150 inch AAT were made using the IDS (Robinson and Wampler 1972) on the Cassegrain spectrograph. The entrance aperture was a square slot subtending 2 arcsec on the sky, and sky background subtraction was accomplished by observing simultaneously through a second entrance slot displaced 1 arcmin on the sky from the first. In some cases, particularly in N86, this "sky" aperture fell on another region of the same nebulosity; in these instances, the [O I] lines could not be accurately measured.

The system response was calibrated, using the standard white dwarf L745-46A (Oke 1974), which is especially valuable as it lacks any obvious absorption features over the whole spectral range observed here, 5500 to 7200 Å.

Integration times were either 4 minutes or 8 minutes; on Figure 1 we show partial scans of a typical high signal-to-noise ratio (S/N) result (in N49) and a more representative result (in 0525−66.0). The comparison between these objects is particularly interesting, since it shows the effect of the large difference in nitrogen abundance between these two objects which is evidenced by the change in the ratio of the [N II] and Hα lines.

The observed line intensities (assuming Hα = 290 on the scale Hβ = 100) without any correction for reddening (which could not be determined for these observations, but which will have only a very small effect on the listed line intensities) are shown in Table 2.

In the western part of N63, the line intensities suggest that we here observed a photoionized nebula; therefore observation has not been included in the discussion that follows.

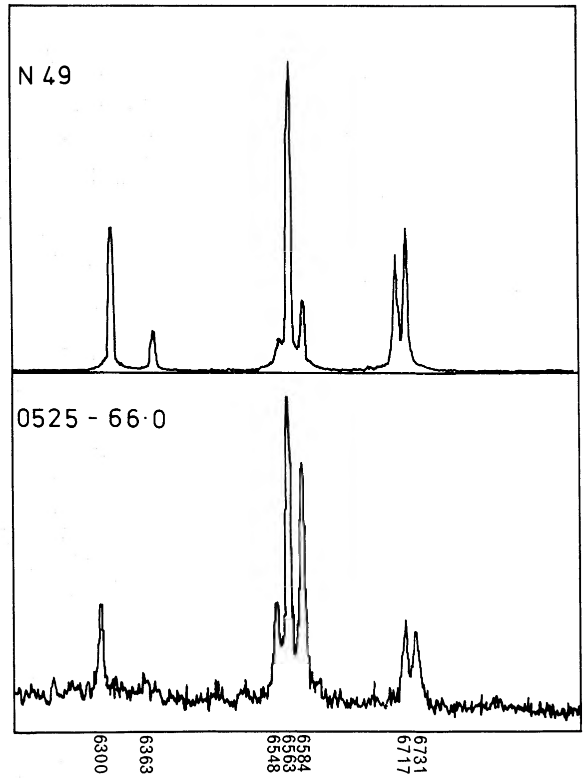

FIG. 1.—Portions of two IDS scans obtained on the AAT. The scan of 0525−66.0 is representative of the quality of the majority of observations. Note the change in Hα/[N II] ratio between the two objects that is an abundance effect.

III. DERIVATION OF ABUNDANCES

The procedure given in Paper II of this series assumes that ideally at least the lines of [O I], [O II], [O III], [N II], and [S II] and the hydrogen lines have been observed. However, in the plate data, because of the high dispersion required to adequately resolve the [S II] lines, the [O II] lines were not observed. In this case, therefore, the oxygen abundance has to be determined from the [O I] lines, which are subject to much larger observational errors. The [O II] lines are taken to have a combined intensity of 7 times the [O I] line at 6300 Å. This is a canonical value derived from the shock models, which, although approximately correct over a large range of abundances and shock conditions, will break down in the limit of high density (which is never reached in these observations) or in the limit of high heavy-element abundance. This latter condition occurs in Pup A, and this case is treated separately. A check on the derived abundance is available, however. The postshock temperature T_2 can be obtained along with the preshock full-preionization density N_1 by using the ratio of the [O III] to the [O I] lines and the ratio of the lines of the [S II] doublet.

The abundances of O, N, and S are derived together from the appropriate diagnostic diagrams in the way described in Paper II. If the abundance of oxygen is known, the ratio of the [O III] λ5007 line to Hβ will furnish a lower limit on the temperature T_2, which can then be compared with that obtained previously. (The limit is lower because increasing carbon abundance weakens the [O III] lines and so, for an appreciable carbon abundance, the implied T_2 will be higher than that derived for zero carbon abundance.) If the oxygen abundance has been underestimated, this lower limit will be higher than the previously derived T_2.

Table 3 shows the abundances derived for the various 74 inch plate objects together with the shock conditions derived for these supernova remnants.

For the data observed on the 150 inch telescope, even greater approximations have to be made. This is because the spectrograph did not have a blue-sensitive image tube, and integration times for lines about 5000 Å wavelength and shorter would become prohibitively long. Thus we have only Hα, the [O I] lines, the [N II] lines, and the [S II] lines. An estimate of density can therefore be made, but we do not have any temperature-sensitive ratio. Fortunately, derived abundances

TABLE 1

SUPERNOVA REMNANT SPECTRA OBSERVED ON THE 74-INCH TELESCOPE

Object		Hβ 4861	[OIII] 4959	[OIII] 5007	[FeII] 5159	[NI] 5200	[OI] 6300	[OI] 6363	[NII] 6548	Hα 6563	[NII] 6584	[SII] 6717	[SII] 6731	Plate quality
Galactic														
Vela X (1)	I	100	23	87	20	20	79	32	62	270	220	167	158	Very good
	Ic	100	23	87	20	20	79	32	62	270	220	167	158	
Vela X (3)	I	100	16	51	12	29	125	30	89	277	262	147	106	Fair
	Ic	100	16	51	12	29	125	30	89	277	262	147	106	
Pupp A	I	100	27	73	30	40	75	37	455	323	1335	147	180	Excellent
	Ic	100	27	72	29	39	68	34	408	290	1200	131	160	
RCW 89 (2)	I	100	53	220	-	≤30	148	65	414	802	1140	580	683	Good
	Ic	100	48	196	-	≲23	60	25	149	290	408	195	230	
RCW 89 (3)	I	100	-	60	-	-	95	45	255	715	790	390	405	Poor
	Ic	100	-	55	-	-	45	20	105	290	335	158	164	
RCW 89 (4)	I	100	33	90	-	-	185	77	341	733	1000	433	510	Fair
	Ic	100	31	82	-	-	85	35	135	290	418	172	201	
W 28 (1)	I	100	33	92	-	-	140	25	92	385	290	215	225	Poor
	Ic	100	33	90	-	-	110	20	70	290	225	163	170	
W 28 (2)	I	100	18	56	-	-	165	50	104	336	285	(210)	190	Fair
	Ic	100	18	55	-	-	145	44	90	290	248	(180)	163	
SMC														
N 19	I	100	29	87	-	-	(22)	(7)	6	293	20	100	83	Good
	Ic	100	29	87	-	-	(22)	(7)	6	290	20	100	83	
N 19 (rpt)	I	100	39	98	-	-	21	8	8	353	21	117	97	Very good
	Ic	100	38	96	-	-	19	7	6	290	18	96	80	

TABLE 2

SUPERNOVA REMNANT SPECTRA IN THE LMC OBSERVED USING THE 150-INCH TELESCOPE

Object	Position (epoch 1975) RA hr min sec	Dec deg min sec	[OI] 6300	[OI] 6363	[NII] 6548	Hα 6563	[NII] 6584	[SII] 6717	[SII] 6731	Notes
N 49	05 25 57.4	-66 06 58	136	40	22	290	66	110	136	Excellent S/N
	05 25 51.0	-66 06 55	87	30	30	290	68	97	112	
	05 25 54.5	-66 06 02	58	21	26	290	79	100	127	
	05 25 47.3	-66 04 30	72	21	27	290	62	67	80	
	05 25 14.9	-66 02 25	58	22	18	290	54	156	101	
	05 24 50.0	-66 02 09	53	17	26	290	61	132	97	
0525-66.0	05 25 26.5	-66 01 09	72	19	97	290	246	93	77	5007/Hβ = 4.0
	05 25 25.5	-66 00 51	50	22	41	290	132	74	91	
	05 25 23.5	-66 00 59	?	?	51	290	120	85	68	
	05 25 17.6	-66 01 57	30?	?	28	290	69	80	86	
NII L	04 54 43.4	-66 28 46	42	12	25	290	61	127	113	
N 63	05 35 38.5	-66 03 24	207	71.6	17.8	290	54.4	164	233	Excellent S/N
	05 35 36.3	-66 03 26	9	3	13	290	41	32	26	Good S/N; photoionised?
N 86	04 55 58.7	-68 42 38	?	?	29	290	63	126	92	
	04 55 53.9	-68 40 38	?	?	16	290	48	96	64	
	04 55 48.9	-68 40 02	?	?	20	290	55	137	75	Poor S/N
	04 55 52.9	-68 43 12	?	?	18	290	48	132	97	
	04 55 37.5	-68 42 49	?	?	17	290	56	117	96	
	04 55 40.3	-68 40 36	35	10	29	290	68	120	82	
	04 55 31.1	-68 41 13	32	12	16	290	44	133	97	Good S/N
N 103 B	05 09 03.5	-68 45 46	99	24	23	290	55	14	29	Very good S/N; 5007/Hβ = 1.1
N 120	05 18 58.4	-69 38 31	28	10	22	290	63	79	70	
N 132 D	05 25 13.3	-69 40 05	53	14	26	290	88	88	120	
0547-69.7	05 47 07.6	-69 42 28	76	25	19	290	57	126	100	
	05 47 36.3	-69 42 13	124	42	20	290	42	185	185	

TABLE 3

PHYSICAL CONDITIONS AND ABUNDANCES IN GALACTIC SUPERNOVA REMNANTS

Object	$\left(\frac{T_2}{10^4}\right)^{\circ}$K*	N_1 cm^{-3}	$\frac{Z(O)}{10^{-4}}$	$\frac{Z(N)}{10^{-5}}$	$\frac{Z(S)}{10^{-6}}$	$\left(\frac{T_2}{10^4}\right)^{\circ}$K†	Ref.
Vela X (1)	9.2	36	1.3	3.9	3.7	8.3	1
" (3)	6.5	≲30	2.5	5.2	3.1	6.0	1
Vela X	8.1	150	1.8	4.5	4.6	6.9	2
Pupp A	7.2	120	6.0	100	25	-	1
RCW 89 (2)	**	≲30	1.1	6.0	5.0	**	1
(3)	9.9	60	0.7	6.7	3.0	9.1	1
(4)	9.0	100	1.6	8.0	5.0	7.9	1
W 28 (1)	10.0	40	2.2	4.5	4.2	7.3	1
(2)	6.8	≲30	3.5	6.0	5.5	5.0	1
Cygnus, 77-1	**	≲30	1.2	4.1	3.5	**	3
IC 418	-	-	1.73	3.2	0.6	-	4

*Obtained from [O III]/[O I] intensity ratio

†Lower limit from [O III]/Hβ intensity ratio

**Lies beyond computed model limits

References:

1 This work; 2 Osterbrock and Costero 1973; 3 Parker 1967; 4 Sandro D'Odorico 1974 (mean value from his filament No. 5, 3, 16, 22, 23, 24, 26 and 31)

TABLE 4

THE OBSERVED DENSITIES AND ABUNDANCES IN THE MAGELLANIC CLOUD SUPERNOVA REMNANTS

Object	N_1 cm^{-3}	$\frac{Z(O)}{10^{-4}}$	$\frac{Z(N)}{10^{-5}}$	$\frac{Z(S)}{10^{-6}}$	Ref.
N 49 (1)	100	3.0	1.4	3.5	1
(2)	90	1.5	1.2	2.5	1
(3)	150	0.9	1.3	2.4	1
(4)	95	1.3	1.0	1.3	1
(5)	≲30	1.0	0.9	2.5	1
(6)	≲30	0.9	1.0	2.2	1
Mean	-	1.4	1.1	2.4	1
N 49	100	1.8	1.6	3.8	2
0525-66 (1)	≲30	1.2	4.0	1.9	1
(2)		0.7	2.0	1.1	1
N 11 L	≲30	0.7	1.0	4.0	1
N 63	250	8.0	2.2	13.0	1
N 86	≲30	0.5	0.8	1.4	1
N 103 B	2000	3.8	0.8	1.1	1
N 120	≲30	0.4	0.8	1.0	1
N 132 D	200	1.4	1.4	2.4	1
0547-69.7 (1)	≲30	1.4	1.0	2.4	1
(2)	40	2.7	1.0	5.5	1
SMC N 19	≲30	0.4	0.21	0.7	1

References:

1 This work; 2 Osterbrock and Dufour 1974

are very insensitive to this quantity, for reasons described in Papers I and II (for example, the ratio [N II] 6584 Å to Hα changes by only 7% at the low-density limit when T_2 varies between 30,000 K and 150,000 K). We therefore adopt a canonical T_2 of 10^5 K.

We consider that likely errors in line intensities given by the models due to uncertain atomic parameters are of the order 25%. Approximations in the modeling lead to at least another 25% to 50% uncertainty. The mean rms error in measuring the important line ratios is about 10%. We therefore expect the error in these abundances to be of order 0.3 in the logarithm and, in the case of oxygen, the probable error in any one determination may be as much as a factor of 0.4 in the logarithm for the IDS measurements but somewhat better than this for the plate data.

Table 4 summarizes the IDS data for all the LMC supernovae observed.

IV. DISCUSSION OF INDIVIDUAL OBJECTS

a) *Vela X*

We consider this object to be well observed with high S/N. Reddening of the remnant appears to be negligible. In fact, the observed strength of Hα is less than its value expected from the shock models by about 7%. For this object, we have excellent photoelectric spectrophotometry by Osterbrock and Costero (1973), who observe an Hα/Hβ ratio of 3.55. We therefore support their conclusion that the very large Hα/Hβ reported earlier by Milne (1968*b*) is not confirmed.

Osterbrock and Costero have also observed all the other lines necessary for a full application of the diagnostic technique, and the derived abundances are also shown on Table 3. These are in close agreement with our values. Furthermore, the postshock temperature T_2 can also be obtained from the ratio of the [O III] and [O II] lines. The value, $T_2 = 74{,}000$ K, agrees well with that obtained from other ratios.

b) *Puppis A*

This object is possibly the most anomalous of the supernova remnants observed.

Optically, it was first described by Baade and Minkowski (1954), and it consists of a few very bright filamentary arris or flocculi. Baade and Minkowski observed most of the brighter flocculi and found [N II] to be very strong with respect to Hα but highly variable from one filament to the next. They were unable to observe other lines. Our observation (which corresponds to their filament No. 3) confirms that the nitrogen lines (including [N I]) are extremely strong in this object. Indeed, the nitrogen is accounting for the majority of the cooling close to the recombination zone, and this can be due only to an overabundance of the element. Since the intensity of a line will tend to saturate at high abundance, this overabundance is much greater than is suggested by simply comparing the ratio of the [N II] lines and Hα in this and other remnants.

The spectrum could not be modeled by any of those previously computed but had to be fitted individually. The result of such a modeling is shown in Table 5.

TABLE 5

COMPARISON OF THE OBSERVED SPECTRUM IN PUPP A WITH A COMPUTED MODEL SPECTRUM (SEE TEXT)

Line		Observed Intensity	Computed Intensity
[O II]	3726	-	323
[O II]	3729	-	262
[O III]	4363	-	3.8
Hβ		100	100.0
[O III]	4959	27	24.0
[O III]	5007	72	72.0
[Fe II]	5158	29	-
[N I]	5200	39	24.0
[O I]	6300	68	29.5
[O I]	6363	34	9.1
[N II]	6548	408	415
Hα	6563	290	290
[N II]	6584	1200	1220
[S II]	6717	131	132
[S II]	6731	160	168

The shock conditions and abundances used in the model are $N_1 = 120\ \mathrm{cm}^{-3}$, $T_2 = 72{,}000$ K, $Z(\mathrm{O}) = 6 \times 10^{-4}$, $Z(\mathrm{N}) = 1.0 \times 10^{-3}$, $Z(\mathrm{S}) = 2.5 \times 10^{-5}$. The absolute values derived from abundances are subject to larger errors than normal, because the heavy elements are all so abundant that they completely dominate the cooling. A very similar spectrum can be obtained if the abundances of these elements are increased in proportion to one another; hence the relative values of the abundances are more accurate than their absolute values. Nevertheless, it is clear that in Pup A, oxygen and sulfur are enriched by factors of at least 2 and nitrogen by at least 10 with respect to other galactic supernova remnants. Since only the ejecta of planetary nebulae approach this sort of enrichment, it is clear that here we observe material belonging to the supernova itself rather than to the shocked interstellar medium with its near-solar abundance.

In this respect, the Pup A flocculi appear to be similar to the filaments of the Crab Nebula (Woltjer 1972) or the "quasi-stationary" knots in Cas A (Peimbert and van den Bergh 1971), although we would hesitate to attempt to apply our shock models to such young supernova remnants as these. Indeed, can the models be applied even to Pup A? We think so, although the flocculi are probably the result of the development of a thermal instability in the expelled supernova material, Regions of higher density cool faster than those of lower density. This results in the development of a low-pressure, high-density zone which is squeezed and further compressed by the high-pressure low-density material about it. Eventually a neutral core may develop in this condensation, with continuing infall, cooling, and compression of the surrounding material. Such a situation in plane-parallel geometry is exactly similar to the shock models, but minus the initial shock heating—the gas having been heated in the initial explosion. Thus the models should be applicable, although the three-dimensionality of the true situation may alter the relative line intensities somewhat.

In the radio, Pup A has been mapped by Milne (1971), who shows poor correlation with the position of the optical flocculi except that they tend to fall near the ridge of radio emission and are clustered toward the northern extreme. The radio object is elongated in the northwest, southeast axis and is very close to the Vel X remnant, which is centered approximately 3° to the southeast. From the radio surface-brightness diameter relationship, the Vel X source is at 0.4 kpc (Woltjer 1972), in good agreement with the optical distance suggested by Milne (1968*a*) on the basis of its apparent interaction with a dark cloud at a distance of 500 pc. Pup A, on the other hand, although it has the same surface brightness as Vel X, is placed at a distance of 1.4 kpc by the same radio technique. Both Pup A and Vel X have similar X-ray spectra (Woltjer 1972), indicating similar physical conditions in the ejecta. Pup A does not show a significantly greater reddening than Vel X, but this result should not be too strongly interpreted, as both objects lie in a relatively unobscured direction in the Galaxy.

The radial velocities of the two objects were measured from the original plates. The local standard of rest (LSR) values obtained with standard deviations are: Vel X, region (1), -14 (± 11) km s^{-1}; Vel X, region (3), $+9$ (± 10) km s^{-1}; Pup A (brightest filament), $+145$ (± 12) km s^{-1}. If we assume that both objects are in circular rotation about the Galaxy, the kinematic distance of Vela is of order 1 kpc, but very uncertain. Pup A, on the other hand, gives a value of 9.6 kpc, or 4 kpc if a mean of Baade and Minkowski's (1954) measurements is used. Both values are inconsistent with either the radio distance or the observed reddening. The dynamics of Pup A are therefore anomalous.

We propose that Pup A and Vel X are at the same distance and form a connected system. Evidence to support this point of view can be seen in Figure 2. Here we have plotted radio isophotes at 2650 MHz for Vel X, Y, and Z (Milne 1968*a*), radio isophotes at 5000 MHz for Pup A (Milne 1971), and all the optical filamentary nebulosity in the two objects taken from photographs (Milne 1968*b*; van den Bergh, Marscher, and Terzian 1973; Baade and Minkowski 1954; Bok 1973). The optical nebulosity can be taken as defining the position of the expanding shock wave in Vela, and is shaped approximately in the form of a D. The center of this nebulosity is marked by a disk, whereas the position of the pulsar, PSR 0833−45 (Large, Vaughan, and Mills 1968), is given by a star in a disk.

The pulsar is displaced from the center of the optical nebula approximately along a line connecting the centers of Vel X and Pup A. This suggests that Pup A has been expelled by the Vela supernova event, the recoil momentum being taken up by the pulsar. If there has been no appreciable braking of Pup A by the interstellar medium—that is, if we assume it to be rather dense, like the fast-moving knots in Cas A—then adopting a mass of 1.5 $M_\odot$ for the pulsar implies a mass of 0.3 $M_\odot$ for Pup A. Since the parent object would certainly have a mass several times the solar value, this estimate leaves plenty of material available as ejecta in the Vel X supernova remnant.

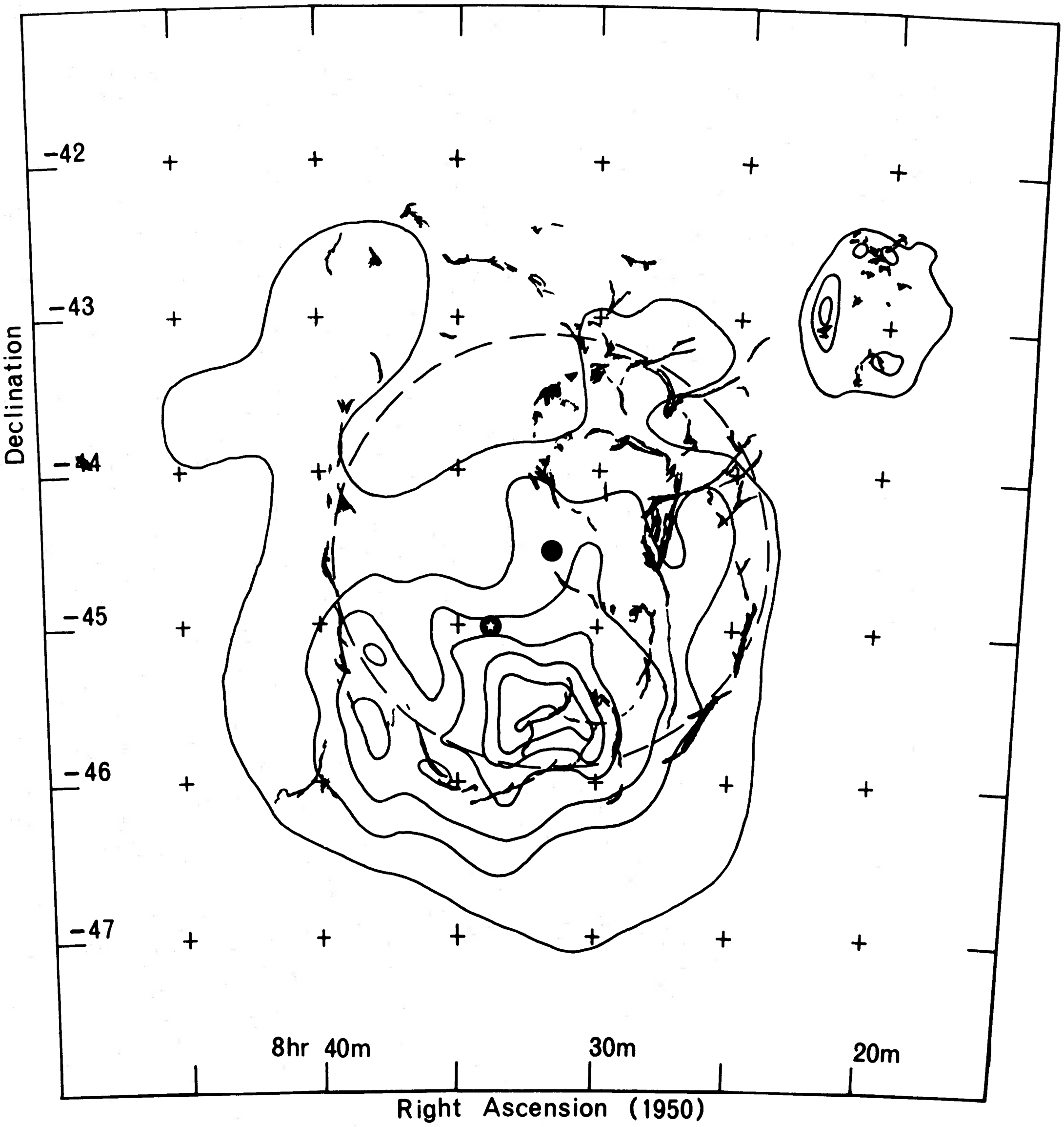

FIG. 2.—A map of the Vela-Puppis region showing evidence for possible ejection of the Puppis source with recoil taken up by the pulsar (star in a disk).

As far as the energetics of the explosion are concerned, Pup A is at a projected distance 17.5 pc from Vel X. The spin-down time for the pulsar, $\frac{1}{2}P(dP/dt)$, is 1.1×10^4 years (Reichley, Downes, and Morris 1970). The mean transverse velocities of Pup A and the pulsar must have been 1560 km s^{-1} and 310 km s^{-1}, respectively, which requires 9×10^{48} ergs of kinetic energy. The total energy involved cannot be much larger than this, because the radial velocity of Pup A is small compared with the transverse velocity. Hence only a few percent of the kinetic energy released in the supernova event are required to eject Pup A to its observed distance.

A possible mechanism for the ejection could have been an asymmetry in the original magnetic field of the pre-supernova star that is amplified along with its pressure term in the collapse or compression of the stellar core.

c) *RCW 89*

Van den Bergh, Marscher, and Terzian (1973) remark that this remnant is located in a region of heavy obscuration, which may account for its low surface brightness. The very heavy reddening observed abundantly confirms this conjecture; we estimate the total extinction at Hβ to lie in the range 3.5 to 4.3 mag. The LSR radial velocity of RCW 89 is found to be -50 (± 12) km s^{-1}, which gives it a kinematic distance of 4 kpc.

d) *W28*

The reddening indicates an extinction at Hβ of around 1 mag.

e) *SMC N19*

This was the only supernova remnant observed in the SMC; as such, it is very interesting. The major feature of the spectrum is the underabundance of all the heavy elements with respect to hydrogen, so that the [N II] lines, for example, are practically invisible. The [O I] lines are very faint, and the ratio of the [O III] to [O I] lines lies outside the range predicted by the shock model. The predicted ratio would be improved if there were an extra cooling process operating in and near the recombination zone. However, as a result of this inconsistency, the oxygen abundance is particularly unreliable; it would be important to observe the [O II] lines in this object and also to obtain spectra of 0046 − 73.5, the other SMC supernova remnant (Mathewson and Clarke 1973*c*).

f) *LMC 0525 − 66.0*

Mathewson and Clarke (1973*a*) have proposed that this source has been ejected from N49 on the basis of their similar nonthermal radio spectra, the fact that its radio emission is too weak for it to be likely to be a supernova remnant in its own right, and the fact that it lies within a more extended region of filamentary nebulosity that extends back to N49.

A more recent prime-focus photograph taken on the 150 inch telescope is shown in Figure 3 (Plate 3). This was a 120-minute exposure on an 098 plate with a RG 630 filter to isolate the Hα, [N II], and [S II] emissions. Here this bridge of material shows up far more clearly. The source 0525 − 66.0 itself shows as a series of bright arris and flocculi, very similar to those in Pup A. In Pup A these cover a total projected length of about 2 pc, but in 0525 − 66.0 the corresponding distance is 22 pc. If the two objects are of a similar nature, therefore, the case of 0525 − 66.0 is altogether more violent both in the size of the fragment and in the distance to which it has been thrown. Again, the fragment has anomalous motions—it is measured to have a velocity of -97 km s^{-1} with respect to N49. Inspection of the observed [N II]/Hα ratios (Table 2) shows also that this object, like Pup A, has a nitrogen abundance anomaly which is highly variable from one point to another. At the most nitrogen-enriched region (Fig. 4 [Pl. 4]), the abundance of the element is observed to be 4 times the mean for N49, whereas at another region there is no significant difference from that observed in N49. The object 0525 − 66.0 is the only object observed in the LMC which has such an anomaly, and we regard this as powerful evidence in support of the ejection hypothesis.

V. OBSERVED ABUNDANCES AND GALATIC ENRICHMENT

The chemical composition of the interstellar medium at a point in time and space is the result of many factors, such as the initial mass function, stellar evolution gas flows, and galactic age.

Pagel (1974) has recently pointed out the importance of observations in the Magellanic Clouds as a means of testing enrichment theories. Important recent reviews of the theories of galactic heavy-element enrichment are those of Talbot and Arnett (1973) and Lynden-Bell (1975). These emphasize the difference between a primary and a secondary nucleosynthesis element. A primary nucleosynthesis element is one with ^{1}H or ^{4}He as its direct progenitor. This class includes C, O, Ne, Mg, Si, S, and Fe. A secondary nucleosynthesis element is one which is produced by subsequent processing of primary elements already present inside the star. The most important of these is ^{14}N, which is produced by the CNO cycle from the primary ^{12}C or (at higher temperatures) from ^{16}O.

Talbot and Arnett (1973) show that the ratio of abundances of any two primary elements i and Z is given by

$$\frac{Z(i)}{Z(z)} = \frac{q_{i1}}{q_{z1}}\,, \tag{1}$$

where the q's are elements of the production matrix that themselves are functions of the initial mass function, stellar evolution, galactic structure, etc. If these are not functions of time, primary elemental abundances increase in proportion to one another.

On the other hand, if k is a secondary species with z its progenitor, then

$$2\,\frac{Z(k)}{Z(z)^2} = \frac{q_{kz}}{q_{z1}}\,. \tag{2}$$

Again, if the production matrix elements are constant, the abundance of a secondary element such as ^{14}N will be proportional to the square of the primary species ^{12}C or ^{16}O. There remains, however, the possibility that ^{14}N can be produced via CNO processing of the C and O made in the star itself (Cameron and Fowler 1971). Such primary production processes will make the dependence of nitrogen abundance less sensitive on the pure primary nucleosynthesis elemental abundances.

Clearly, then, the nitrogen abundance is a sensitive indicator of the degree of secondary processed material that has been recycled into the interstellar medium. Evidence of an underabundance of nitrogen in the planetary nebulae of Magellanic Clouds was first obtained from objective prism spectra by Sanduleak, MacConnell, and Hoover (1972), and many data have recently become available confirming this trend in the H II regions of both Magellanic Clouds (Peimbert and Torres-Peimbert 1974; Dufour 1975; Smith 1975).

Our observations of the abundances in the shocked interstellar medium both confirm and extend this trend. In Table 6 we give the mean elemental abundances found in the LMC, the SMC, and our Galaxy. The two objects, Pup A and 0525 − 66.0, are excluded from these means for reasons that should be obvious from our earlier remarks.

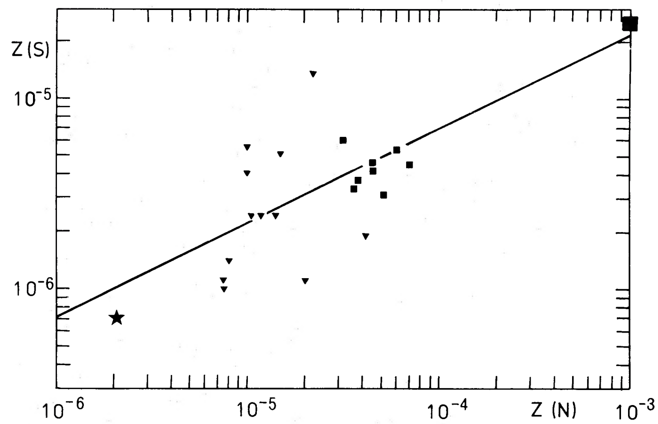

FIG. 5.—The correlation between S and N abundances. The SMC object N19 is a star, LMC objects are triangles, and galactic objects are squares.

In Figure 5 the sulfur abundance is plotted on logarithmic scales by number, $Z(\mathrm{S})$, against the nitrogen abundance $Z(\mathrm{N})$, which shows clearly the trend from SMC (*star*) to LMC (*triangles*) to Galaxy (*squares*) to Pup A (*square at extreme right*). The line drawn is not a least-squares fit, but a line of slope $\frac{1}{2}$ which is the theoretical value if nitrogen is a pure secondary nucleosynthesis element. Hence there is no observational evidence to support the idea that primary production of nitrogen plays a significant role. This can be observed if one looks at Figure 6, where the relation between oxygen and nitrogen abundance is plotted. All the supernova remnants observed are shown as squares on this diagram. The correlation between the abundances is extended and improved when all the high-quality data from planetary nebulae are included (*triangles*). Such a relationship between oxygen and nitrogen abundances was noted very recently by D'Odorico, Peimbert, and Sabbadin (1976); and in Figure 6 we have included data from the following sources; Peimbert and Torres-Peimbert (1971); Miller (1969); Peimbert (1973); Buerger (1973); and Boeshaar (1975).

We also plot on Figure 6 the abundances derived from the theoretical values given by Talbot and Arnett (1973) according to three different scenarios of enrichment which they label I, IIA, and IIB. The exact value of the production matrix elements is very sensitive to the initial mass function (IMF) of the stars. This can be parametrized by the relation

$$N(m) = Cm^{-m} \tag{3}$$

where $N(m)$ is the number of stars of mass m. We have selected the value of μ (1.8) which gives the largest range of enrichment in the models, so that the difference between I and IIB is roughly the range of theoretically allowed values. These observations suggest that IIB is the most plausible.

The fact that SMC N19 fits on the correlation so well means that the oxygen and sulfur abundances [$Z(0) = 0.4 \times 10^{-4}$, $Z(\mathrm{S}) = 0.7 \times 10^{-6}$] observed in this object furnish upper limits on the primordial abundance of these elements in the precollapse gas which formed our Galaxy. Furthermore, the lack of evidence of any curvature in the correlation above the errors implies that there has not been any very strong evolution in enrichment processes during the evolution of these local galaxies either through time or through their chemical evolution.

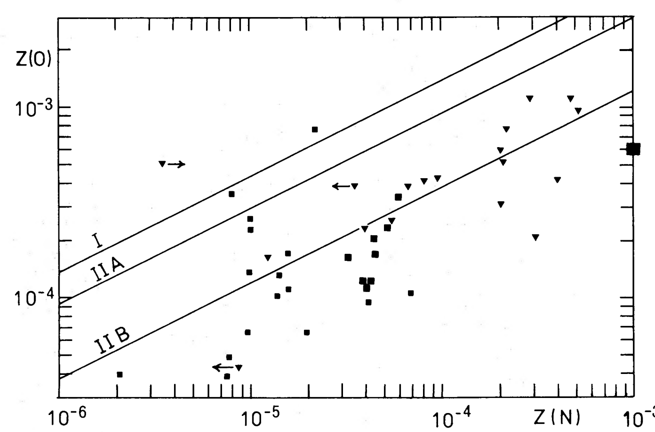

FIG. 6.—The correlation between O and N abundances for supernova remnants (*squares*) and planetary nebulae (*triangles*)

TABLE 6

COMPARISON OF MEAN ELEMENTAL ABUNDANCES IN THE THREE GALACTIC SYSTEMS

System		$Z(O)/10^{-4}$	$Z(S)/10^{-6}$	$Z(N)/10^{-5}$
Galaxy	(5 objects)	1.8	3.8	5.2
LMC	(8 objects)	2.2	2.5	1.2
SMC	(1 object)	0.4	0.7	0.2

It is very interesting to compare these results on shocked interstellar gas with the other source of abundances in the interstellar medium in other galaxies, the H II regions. In Figure 7 we have plotted all the data available, without selection, from the following sources: Peimbert and Costero (1969); Searle (1971); Dopita (1973, 1974); Simpson (1973); Peimbert and Torres-Peimbert (1974); Dufour (1975); and Smith (1975). The data, although spread over many galaxies, form a very tight correlation, with a slight suggestion of curvature between Talbot and Arnett's versions I and IIA, and appear to be systematically different from the supernova values.

Is there therefore a real disagreement between the two ways of deriving abundance? Before opening such a discussion, we would like to remind readers that there is a factor of 2 uncertainty in the supernova abundances which of itself can account for much of the apparent difference. However, we believe that there may also be a systematic error affecting most of the observations shown in Figure 7.

Consider for a moment only the case of the Orion Nebula, a key object in the understanding of H II regions. Observations on this object, regrettably, show the greatest scatter in abundance determinations. Peimbert and Costero (1969) and Peimbert and Torres-Peimbert (1974) obtain $Z(\mathrm{O})$ close to 8×10^{-4} and $Z(\mathrm{N})$ near 5×10^{-5}. Dopita (1974) and Simpson (1973), using different techniques, find $Z(\mathrm{O})$ in the vicinity of 2.5×10^{-4} and $Z(\mathrm{N})$ near 3.5×10^{-5}. The technique adopted by Peimbert and Costero, in which the importance of line-of-sight temperature variations was recognized, has been virtually universally accepted and has been used by all other authors whose work is shown on Figure 7, so we expect any systematic error which may affect the results to operate equally on all and bodily shift the curve.

We believe that such a systematic error may well have been caused by a systematic temperature difference between the low-ionization zone emitting O^+, N^+, and S^+ radiations and the zone emitting O^{++} and S^{++} lines. A systematically higher temperature in the low-ionization zone is expected on three theoretical grounds. We know that H II regions are likely to contain many neutral inclusions surrounded by (probably) D-type ionization fronts (Dopita, Dyson, and Meaburn 1974; Dopita, Isobe, and Meaburn 1975). In such a situation, ionized gas flowing off these inclusions will be denser than the mean, resulting in collisional de-excitation (of the [O II] lines in particular) and consequent higher equilibrium temperature. Furthermore, the gas passing through the ionization front will tend to become superheated because of a lag between the heat input and its subsequent loss owing to the state of ionization of the gas being lower than its equilibrium value. Third, the radiation field close to the inclusion will be hard because of the preferential absorption of the softer UV radiation closer to the exciting star (Hummer and Seaton 1964).

Observational evidence for such a systematic difference in temperature appears in Peimbert and Costero's (1969) paper directly, but their analysis is made on the assumption of uniform temperature. This appears to produce a trend in the oxygen abundance from high-excitation regions to low-excitation regions. Simpson (1973) relied on measurement of the ratio of Hβ to the Balmer continuum to derive temperatures, and found little change of the observed abundance with changing excitation.

Dopita (1973) used a totally different technique based on measurement of the ratio of [O III] to Hβ and of [N II] to Hα. Such ratios are independent of reddening and were shown to be also independent of temperature fluctuations along the line of sight. Measurements at many points in the nebula coupled

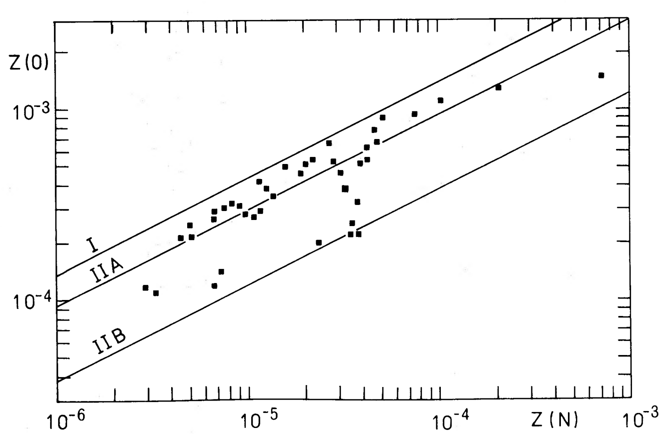

FIG. 7.—As Fig. 6, but for H II regions

with an independent temperature determination make it possible to separate temperature and ionization effects and find a mean abundance of nitrogen and oxygen. This technique proved the existence of an inverse correlation between temperature and ionization and gave lower abundances than the Peimbert and Costero technique.

To conclude, then, there are grounds for supposing that the apparent discrepancy between H II region and supernova determinations of O and N abundances may not be real, owing to systematic effects produced by the techniques, but these difficulties do not make it possible to select a model of enrichment. All that can be said with confidence is that primary production of nitrogen appears to be unimportant, and time- or enrichment-dependent factors in the enrichment processes are not overwhelming. No evidence for a significant primordial abundance of oxygen or sulfur has been found.

A significant increase in the interstellar oxygen and sulfur abundance and (even more so) in nitrogen abundance has been confirmed by a totally new technique in the sense of SMC to LMC to our Galaxy. This may be a consequence of the greater gas mass to stellar mass in the SMC compared with the LMC compared with our Galaxy.

REFERENCES

Baade, W., and Minkowski, R. 1954, *Ap. J.*, **119**, 206.
Boeshaar, G. O. 1975, *Ap. J.*, **195**, 695.
Bok, B. J. 1973, in *The Gum Nebula and Related Problems* (NASA SP-332), p. 148.
Brocklehurst, M. 131, *M.N.R.A.S.*, **153**, 471.
Buerger, E. G. 1973, *Ap. J.*, **180**, 817.
Cameron, A. G. W., and Fowler, W. A. 1971, *Ap. J.*, **164**, 111.
Cox, D. P. 1972, *Ap. J.*, **178**, 143.
D'Odorico, S. 1974, in *Supernovae and Supernova Remnants*, ed. C. B. Cosmovici (Dordrecht: Reidel), p. 283.
D'Odorico, S., Peimbert, M., and Sabbadin, F. 1976, *Astr. Ap.*, **47**, 341.
Dopita, M. A. 1973, *Astr. Ap.*, **29**, 387.
———. 1974, *Astr. Ap.*, **32**, 121.
———. 1976, *Ap. J.*, **209**, 395 (Paper I).
———. 1977, *Ap. J. Suppl.*, **33**, 437 (Paper II).
Dopita, M. A., Dyson, J. E., and Meaburn, J. 1974, *Ap. Space Sci.*, **28**, 61.
Dopita, M. A., Isobe, S., and Meaburn, J. 1975, *Ap. Space Sci.*, **34**, 91.
Dufour, R. J. 1975, *Ap. J.*, **195**, 315.
Hummer, D. G., and Seaton, M. J. 1964, *M.N.R.A.S.*, **127**, 217.
Large, M. I., Vaughan, A. E., and Mills, B. Y. 1968, *Nature*, **220**, 340.
Lynden-Bell, D. 1975, *Vistas in Astronomy*, **19**, 299.
Mathewson, D. S., and Clarke, J. N. 1973*a*, *Ap. J.*, **179**, 89.
———. 1973*b*, *Ap. J.*, **180**, 725.
———. 1973*c*, *Ap. J.*, **182**, 697.
Miller, J. S. 1969, *Ap. J.*, **157**, 1215.
Milne, D. K. 1968*a*, *Australian J. Phys.*, **21**, 201.
———. 1968*b*, *Australian J. Phys.*, **21**, 501.
———. 1971, *Australian J. Phys.*, **24**, 429.
Oke, J. B. 1974, *Ap. J. Suppl.*, No. 236, **27**, 21.
Osterbrock, D. E., and Costero, R. 1973, *Ap. J.* (*Letters*), **184**, L71.
Osterbrock, D. E., and Dufour, R. J. 1973, *Ap. J.*, **185**, 441.
Pagel, B. E. J. 1974, *ESO/SRC/CERN Conference on Large Telescopes*, ed. A. Reiz (Geneva: European Southern Observatory), p. 131.
Parker, R. A. R. 1967, *Ap. J.*, **149**, 363.
Peimbert, M. 1973, *Mém. Soc. Roy. de Liège*, 6e sér., **5**, 307.
Peimbert, M., and Costero, R. 1969, *Bol. Obs. Tonantzintla y Tacubaya*, **5**, 3.
Peimbert, M., and Torres-Peimbert, S. 1971, *Ap. J.*, **168**, 413.
———. 1974, *Ap. J.*, **193**, 327.
Peimbert, M., and van den Bergh, S. 1971, *Ap. J.*, **167**, 223.
Reichley, P. E., Downes, G. S., and Morris, G. A. 1970, *Ap. J.* (*Letters*), **159**, L35.
Robinson, L., and Wampler, E. J. 1972, *Pub. A.S.P.*, **84**, 161.
Sanduleak, N., MacConnell, D. J., and Hoover, P. S. 1972, *Nature*, **237**, 28.
Searle, L. 1971, *Ap. J.*, **168**, 327.
Simpson, J. P. 1973, *Pub. A.S.P.*, **85**, 479.
Smith, H. E. 1975, *Ap. J.*, **199**, 591.
Talbot, R. J., Jr., and Arnett, W. D. 1973, *Ap. J.*, **186**, 51.
van den Bergh, S., Marscher, A. P., and Terzian, Y. 1973, *Ap. J. Suppl.*, No. 227, **26**, 19.
Woltjer, L. 1972, *Ann. Rev. Astr. Ap.*, **10**, 129.

M. A. DOPITA, V. L. FORD, and D. S. MATHEWSON: Mount Stromlo and Siding Spring Observatory, Private Bag, Woden P.O., A.C.T., Australia, 2606

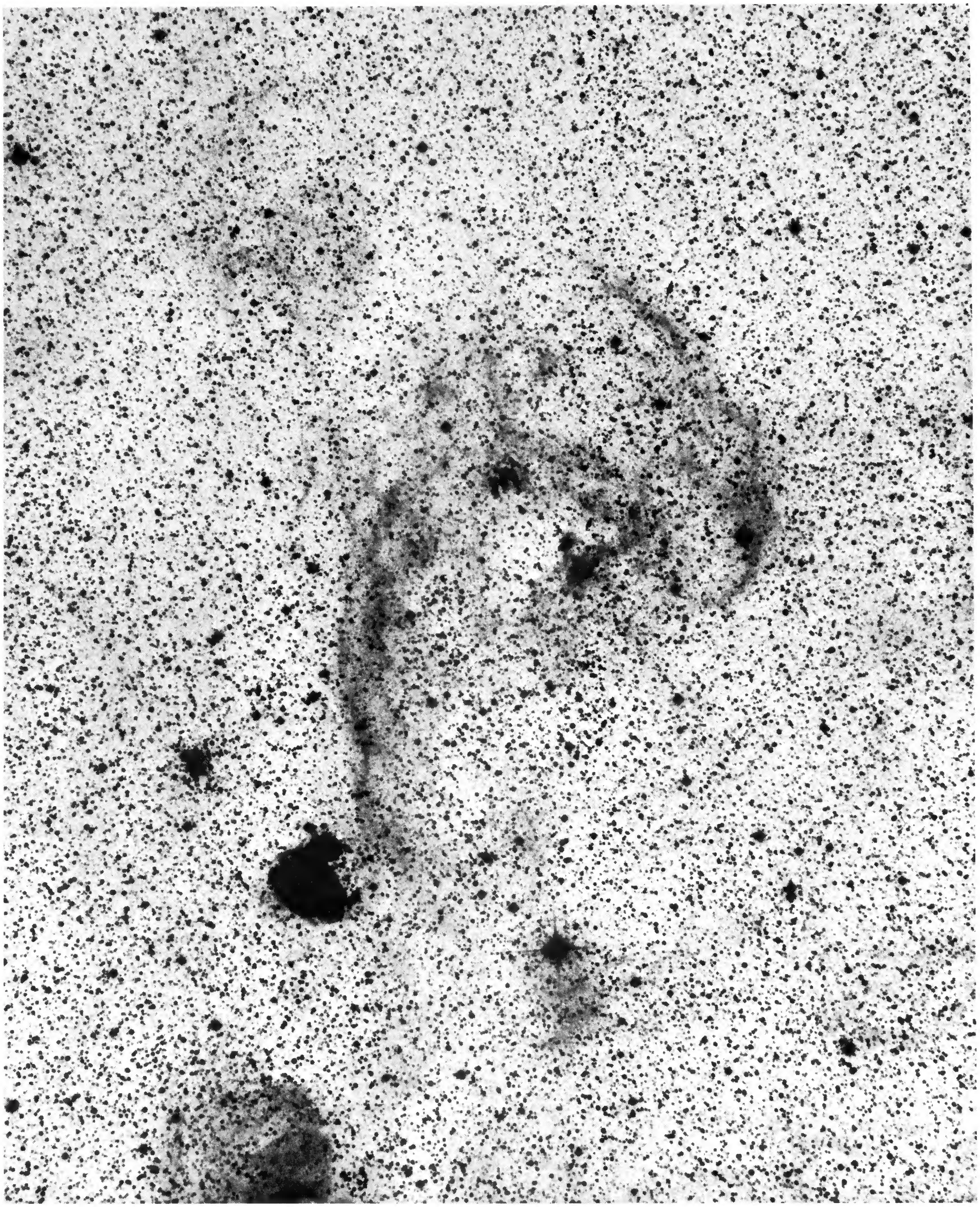

FIG. 3.—150 inch prime focus of N49 (*black "duck"-shaped object, lower left*), 0525 – 66.0 ("*m*"-*shaped system of filaments, upper center*), and the extended nebulous bridge linking them. For details of exposure, see text.

DOPITA *et al.* (*see* page 185)

FIG. 4.—150 inch prime focus photograph of the supernova remnant N86 (the "Lionel-Murphy" SNR)

DOPITA *et al.* (*see* page 185)